

AperTO - Archivio Istituzionale Open Access dell'Università di Torino

Seasonal variation of soil physical properties under different water managements in irrigated rice

This is the author's manuscript

Original Citation:

Availability:

This version is available <http://hdl.handle.net/2318/90919> since 2017-05-27T07:43:52Z

Published version:

DOI:10.1016/j.still.2011.10.011

Terms of use:

Open Access

Anyone can freely access the full text of works made available as "Open Access". Works made available under a Creative Commons license can be used according to the terms and conditions of said license. Use of all other works requires consent of the right holder (author or publisher) if not exempted from copyright protection by the applicable law.

(Article begins on next page)



UNIVERSITÀ DEGLI STUDI DI TORINO

1
2
3
4
5
6
7
8
9
10
11
12
13

This is an author version of the contribution published on:

Questa è la versione dell'autore dell'opera:

*[**Soil and Tillage Research**, 118, 2012, Pages 22-31, doi:
10.1016/j.still.2011.10.011]*

The definitive version is available at:

La versione definitiva è disponibile alla URL:

*[**<http://www.sciencedirect.com/science/article/pii/S0167198711001772>**]*

14 Title: SEASONAL VARIATION OF SOIL PHYSICAL PROPERTIES UNDER
15 DIFFERENT WATER MANAGERMENTS IN IRRIGATED RICE

16

17 Author names and affiliations: Dario Sacco¹, Cassiano Cremon², Laura Zavattaro¹, Carlo
18 Grignani¹

19

20 ¹Department of Agronomy, Forestry and Land Management – University of Turin- via L. Da
21 Vinci 44, 10095 Grugliasco (TO) - ITALY

22 ² Departamento de Agronomia - Ciência do Solo. UNEMAT - Universidade do Estado de
23 Mato Grosso. Av. São João s/n – Bairro Cavahada, CEP: 78200-000 - Cáceres-MT -
24 BRAZIL

25

26 Corresponding author:

27 Dario Sacco, Department of Agronomy, Forestry and Land Management – University of
28 Turin- via L. Da Vinci 44, 10095 Grugliasco (TO) – ITALY. Tel.: +390116708787, Fax:
29 +390116708798, email: dario.sacco@unito.it.

30

31

32 Title: SEASONAL VARIATION OF SOIL PHYSICAL PROPERTIES UNDER
33 DIFFERENT WATER MANagements IN IRRIGATED RICE

34

35 Abstract

36 While soil porosity and soil hydrological properties are key characteristics that define
37 different soil types, they are influenced by many factors: land use, tillage management, and
38 agricultural practices such as irrigation. As expected, water management impacts the physical
39 properties of soil in irrigated rice significantly; however, the importance of seasonal variation
40 on those soil properties requires further consideration, especially given the period of
41 continuous submersion. In this paper, the different soil physical properties have been studied
42 with two goals in mind: 1) to compare the bulk densities, cumulative pore size distribution
43 curves, and near-saturated hydraulic conductivity values associated with seasonal variation
44 induced by submerging water or rainfall on irrigated rice cultivated under two different water
45 managements and in one rain-fed crop, and 2) to describe and parameterize the relationship
46 that links near-saturated hydraulic conductivity to soil porosity in a generic semi-empirical
47 model independent of treatment differences and seasonal variability.

48 The experiment was conducted in the Piedmont Region (NW Italy) in sandy loam soil on
49 three contiguous fields cultivated as follows: (i) continuous rice in submersion, (ii) continuous
50 rice seeded in dry soil submerged one month after the first field, and (iii) maize in rotation
51 with rice (rain-fed treatment). The physical properties of the soil were measured five times
52 over the year at depths of 0-12 cm and 12-25 cm.

53 Results showed a progressive compaction of the soil and a consequent reduction of the near-
54 saturated hydraulic conductivity due to submersion. Macro- and meso-porosity decreased
55 while micro-porosity increased. At the end of submersion, new large porosity was created and
56 the situation reverted to that noted at the start of the year. The non-submerged field showed a

57 different behaviour; in the absence of submersion, bulk density reduced as a result of rainfall
58 but the effect on the different classes of pores was reversed.

59 Finally, a new semi-empirical model is presented that describes near-saturated hydraulic
60 conductivity as a function of soil porosity.

61 Key words: rice; irrigation; soil porosity; soil physical properties; semi-empirical model.

62

63 1 Introduction

64 The relationship between soil physical properties and soil structure and porosity has been
65 widely explained by Kutilek (2004). The author classified soil pores according to their
66 hydrological functionality: (i) submicroscopic pores are considered non-active; (ii) micro-
67 pores (capillary pores) are those where the unsaturated flow of water occurs; (iii) macro-pores
68 (non-capillary pores) are those where capillary menisci are not formed across the pore and
69 water flow is driven by gravity alone. Other authors have introduced the concept of meso-
70 porosity (Luxmoore, 1981) as pores having an intermediate functionality between macro- and
71 micro-porosity.

72 Other than hydrology, soil porosity influences biogeochemical processes and soil fertility. For
73 example, pore size distribution, together with pore shape and connectivity, influences the
74 transport of dissolved and non-dissolved chemicals and gases. It also acts upon plant rooting
75 and on the conditions for the life of all soil biota (Kutilek et al., 2006). Furthermore, it helps
76 explain the dynamics of soil C and N cycles (Juma, 1993) and is positively correlated with
77 root growth and soil enzyme activity (Pagliai and De Nobili, 1993). Clearly its description is
78 of primary import in agricultural systems.

79 Soil porosity can be described using direct methods based on microscopic techniques and
80 image analyses (Pagliai and Vignozzi, 2002) or it can be described functionally using indirect
81 methods based on the measurement of soil physical properties. A functional description of
82 porosity requires the estimation of total soil porosity by pairing bulk densities with particle
83 densities, the distribution of pore size in the soil by utilizing the water retention curve, and the
84 identification of those soil pores that are highly active in water and solute transmission by
85 measuring the near-saturated hydraulic conductivity (Ankeny et al., 1991).

86 Soil porosity and soil hydrological properties characterize the different types of soils, but are
87 also largely influenced by land use (Bormann and Klaassen, 2008), tillage management,

88 (Moret and Arrùe, 2007a) and other agricultural practices. Moreover, they change over time
89 due to anthropic soil perturbation and environmental forces. For example, as reported by
90 Cameira et al., (2003) in a maize cultivation experiment, irrigation affected the macro-
91 porosity and meso-porosity of the ploughed layer as evidenced by a decrease of 65% and
92 50%, respectively. This was attributed to the breakdown of fragile pores created by tillage.
93 Furthermore, in the same experiment, seven irrigation events were found to effect a
94 continuous reduction in macro-porosity until harvest when it increased, probably due to root
95 development.

96 Many have described the effect of wet–dry cycles on soil porosity and consequently, on soil
97 physical properties (Petersen et al., 2004; Schwartz et al., 2003). Additionally, many have
98 focused on describing the soil physical property dynamics of irrigated rice under different
99 puddling intensities and depths compared to unpuddled fields (Kukul and Aggarwal, 2002;
100 Mohanty et al., 2004). They have demonstrated that the continuous presence of submerging
101 water destroys porosity and reduces water percolation in treatments where puddling is not
102 applied. However, description of the effect of submerging water on different soil physical
103 properties as opposed to rainfall on rain-fed crops remains unexplored.

104 The description of the dynamics of the different soil hydrological properties can be simplified
105 by the fact that some of them vary together. In particular, authors have related the near-
106 saturated hydraulic conductivity to the amount of pores hydraulically active (Kozeny, 1927,
107 Carman, 1937 and 1956, Aimrun et al., 2004). Consequently, the near-saturated hydraulic
108 conductivity dynamic—a time consuming measurement—can be described using other easier-
109 to-measure variables, such as the dynamic of total soil porosity.

110 The different soil physical properties considered in this paper have been studied with two
111 goals: 1) to compare the bulk densities, cumulative pore size distribution curves, and near-
112 saturated hydraulic conductivity values associated with seasonal variation induced by

113 submerging water or rainfall on irrigated rice cultivated under two different water regimens
 114 and in one rain-fed crop, and 2) to describe and parameterize the relationship that links near-
 115 saturated hydraulic conductivity to soil porosity in a generic semi-empirical model
 116 independent of treatment differences and seasonal variability.

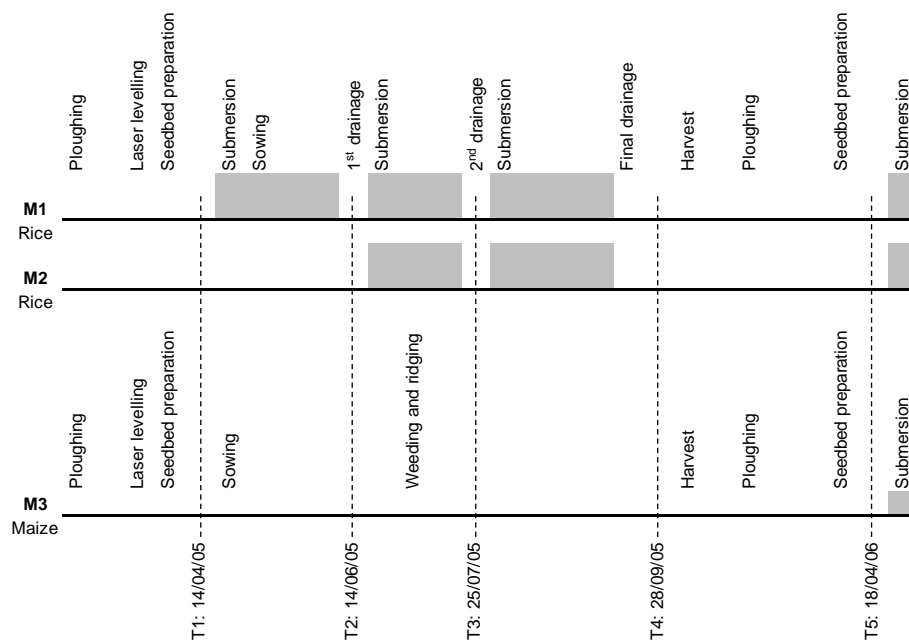
117

118 2 Materials and methods

119 The experiment was carried out in 2005 in the Piedmont Region (NW Italy, lat. 45° 17', long.
 120 8° 25') in the widest European paddy area on a Typic Endoaquept, coarse-silty, mixed, non-
 121 acidic, mesic soil (USDA, 1977). The explored horizon (0-25 cm) was classified as sandy
 122 loam according to USDA texture classification. The average soil organic carbon content was
 123 9.8 g kg⁻¹ dry soil.

124 We analysed the physical properties of the soil in three contiguous fields totalling about 1840
 125 m², hydraulically separated by 80 cm large embankments, and supplied with water derived
 126 from the same channel.

127



128

129 Fig. 1: Samplings and managements of the three fields in the experiment.

130 The three fields differed in that each underwent a unique water management described in
131 Figure 1. The first management (M1) was based on continuous rice (*Oryza sativa* L.)
132 submerged from before seeding up to one month before harvest with two drainages of about
133 five days each; it represented the traditional management of the area. In the second (M2), rice
134 was seeded in dry soil and irrigation was delayed for one month later than in the M1 field.
135 The third (M3) field was cultivated with maize (*Zea mays* L.) after two years of continuous
136 rice; it served as the experimental control as it never received irrigation during the studied
137 year.

138 All three fields were ploughed in spring with a moldboard plough and laser levelled. The
139 seedbeds were prepared using a rotovator. Additionally, the maize crop was weeded and
140 ridged two months after sowing. Although puddling is a common practice in paddy areas
141 around the world, it is not done in the Italian paddy area and consequently, not in our fields.

142 In each field, measurements were taken from two different holes dug about 5 m apart and
143 placed in the centre of the field.

144 The three fields were physically characterised at the start of the experiment from soil texture
145 and particle density measurements. Soil texture was measured using the pipette method
146 according to SIA (2000) on 25g samples. Measurements were replicated six times for each
147 field. Particle density (PD) was measured using 20g samples for six replications on each field
148 via the picnometer method (Blake and Hartge, 1986a) utilising ethylic alcohol as the
149 displaced fluid (EMBRAPA, 1997).

150 The resulting measurements showed that the different fields were generally homogeneous
151 (Table 1). Differences appeared in the coarse sand of the first layer (5%) and in the clay of the
152 second layer (1.7%). However, as they were not too large, we considered that they would not
153 influence hydrological properties.

154

155 Table 1: Average values and 95% confidence intervals of the physical parameters of the soil.

Parameter	MU	T1		T2		T3	
		0-12 cm	12-25 cm	0-12 cm	12-25 cm	0-12 cm	12-25 cm
Clay	%	6.5 ± 1.8	6.9 ± 1.1	6.3 ± 1.1	6.6 ± 1.0	5.0 ± 1.0	5.2 ± 0.6
Fine silt	%	20.0 ± 2.3	19.7 ± 2.5	21.5 ± 0.8	21.6 ± 1.7	20.3 ± 0.8	19.7 ± 1.9
Coarse silt	%	22.1 ± 2.5	25.0 ± 2.6	24.5 ± 1.1	24.8 ± 2.5	24.8 ± 3.0	24.8 ± 2.8
Fine sand	%	26.9 ± 2.0	27.7 ± 2.4	27.6 ± 1.2	27.5 ± 3.8	28.6 ± 3.5	31.0 ± 4.6
Coarse sand	%	24.5 ± 2.4	20.8 ± 2.5	20.1 ± 0.4	19.5 ± 0.8	21.2 ± 1.0	19.3 ± 2.4
Particle density	Mg m ⁻³	2.57 ± 0.07	2.59 ± 0.09	2.62 ± 0.04	2.60 ± 0.07	2.59 ± 0.06	2.58 ± 0.08

156

157 2.1 Repeated soil physical measurements

158 We repeated the following soil measurements at different times during the experiment: soil
159 dry bulk density, water retention curve, and near-saturated hydraulic conductivity curve.

160 The cylindrical sampler method (Blake and Hartge, 1986b) was used to measure soil dry bulk
161 density (BD) with six replicates for each field measurement. The cores were 50.4 mm in
162 diameter and 50.0 mm high (100 cm³). The total porosity (Φ) was derived from the BD and
163 PD through the known function:

$$164 \quad \Phi = 1 - \frac{BD}{PD} \quad [1]$$

165 The water retention curve was derived in the laboratory from undisturbed samples.
166 Laboratory analyses were conducted in desorption, with both tension chamber and
167 pressure plate apparatuses, following the methodology proposed by Klute (1986). Three
168 cylindrical soil samples (58 mm in diameter and 30 mm in height) were extracted, weighed at
169 saturation and after equilibration at various pressures, and then oven-dried (105 °C, 24
170 hours) to determine their dry weight. Water tensions of 0.2, 0.5, 1, 2, 5, 6, and 10 kPa were
171 achieved in a tension chamber while water tension of 33 kPa was achieved in the pressure
172 plate apparatus. The soil samples used for determining the water retention curve were
173 thinner and larger than those used for determining soil bulk density. The thinner samples
174 accelerate attaining equilibrium *versus* the hydrological equipment as water has a shorter

175 pathway to leave the sample. Since thinner soil samples cause the volume determination to
176 be less precise because of the roughness of the two surfaces, we expressed the water content
177 first as water content relative to saturation of each sample, then converted it to absolute
178 water content via the soil total porosity calculated using equation [1]. The results of the
179 water retention curve were converted to a cumulative pore size distribution. The equation
180 reported by Gardner et al. (1991) was used to calculate the equivalent pore radius of the
181 pores corresponding to the different water tension values. The measured water content was
182 considered to be the total volume of pores occupied by water at each tension and represents
183 the sum of the volume of all pores filled with water at a given tension.

184 The near-saturated hydraulic conductivity was measured in four replicates for each field
185 measurement using tension infiltrometers (White, 1992) with 148 mm diameter bottoms.
186 The steady-state infiltration rate was measured at each location manually at three different
187 water tensions (0.05, 0.1 and 0.2 kPa). The measurements started at the highest water tension
188 and ended with the lowest (i.e., closest to saturation) in order to avoid problems due to
189 hysteresis (Zavattaro et al., 1999). The infiltrometers were directly placed over the soil
190 without any interposed material. The steady-state infiltration rate was converted from three-
191 dimensional hydraulic conductivity into one-dimensional hydraulic conductivity following
192 the method proposed by Ankeny *et al.* (1991). With this procedure, involving linear
193 interpolation between measurements, four pairs of hydraulic conductivity at water tensions
194 of 0.05, 0.075, 0.15, and 0.2 kPa were calculated and the value corresponding to the mid
195 water tensions was removed (0.1 kPa). This procedure, based on a stepwise interpolation,
196 has been widely applied by other authors (Messing and Jarvis, 1993; Zavattaro et al., 2001;
197 Daraghmeh et al., 2008).

198 Following this set of measurements and according to the literature, macro-porosity was
199 defined as pores with an equivalent radius of greater than 745 μm applying a water tension

200 equivalent to 0.2 kPa (adapted from Cameira et al., 2003) while the upper limit of micro-
201 porosity was chosen as 30 μm per Kutilek (2004), which corresponds to a water tension
202 equivalent to 2 kPa. Consequently, meso-porosity was defined in the range of 0.2-2 kPa.

203 2.2 Measurements times and depths

204 The bulk density, cumulative pore size distribution, and near-saturated hydraulic conductivity
205 were each measured in the three fields at five different times corresponding to the rice
206 management operations reported in Figure 1:

- 207 1) after seedbed preparation and before the first submersion of M1 (T1 = 14/04/2005);
- 208 2) upon initial drainage of M1 and immediately before the first submersion of M2 (T2
209 = 14/06/2005);
- 210 3) at the second drainage of M1 corresponding to the first drainage of M2 (T3 =
211 25/07/2005);
- 212 4) after the final and complete drainage of M1 and M2 (T4 = 28/09/2005);
- 213 5) at seedbed preparation during the following year, (T5 = 18/04/2006).

214 In M3, weeding and ridging occurred between T2 and T3.

215 The measurements were conducted in the ploughed layer at 0-12 cm and 12-25 cm which
216 allowed for evaluation of the effect of the submerging water on the two depths. The
217 cumulative pore size distribution curve was not measured in the first layer at T1 and T5 as the
218 soil was too incoherent to allow undisturbed sampling. Moreover, measurements were not
219 performed in the second layer at T2 and T3 because it was impossible to dig holes in the
220 fields during short-term drainage due to the high water content. Details of the measurements
221 are reported in Table 2.

222

223

224 Table 2: Measurements performed at different times and in different soil layers for each
 225 attribute analysed on the three fields.

Measurement	Time	Depth		
		0 - 12 cm	12 - 25 cm	
Bulk Density	Start	T1	X	X
	1 st drying	T2	X	
	2 nd drying	T3	X	
	Final	T4	X	X
	2 nd year	T5	X	X
Water Retention Curve	Start	T1	X	
	1 st drying	T2	X	
	2 nd drying	T3	X	
	Final	T4	X	X
	2 nd year	T5		X
Near-saturated hydraulic conductivity	Start	T1	X	X
	1 st drying	T2	X	
	2 nd drying	T3	X	
	Final	T4	X	X
	2 nd year	T5	X	X

226

227 2.3 Data analysis

228 2.3.1 Seasonal variations

229 The seasonal variation in the bulk density, cumulative pore size distribution, and near-
 230 saturated hydraulic conductivity at different water tensions were analysed to compare the
 231 effect of the different water managements. Data on the near-saturated hydraulic conductivity
 232 at different water tensions showed a log-normal distribution as reported by other authors
 233 (Petersen et al., 2004); afterwhich, they were presented as log-transformed data. As variances
 234 were not homogeneous between different water managements, the 95% confidence intervals
 235 were chosen to allow the independent comparison between treatments. Only means showing
 236 significant differences are discussed here.

237

238 2.3.2 Porosity—near-saturated hydraulic conductivity relationship

239 The relationship between saturated hydraulic conductivity and soil porosity is largely known
 240 (Ahuja et al., 1984; Messing, 1989; Rawls et al., 1998; Aimrun et al., 2004; Han et al., 2008)
 241 and described through a power function parameterised with two empirical constants that are
 242 site specific. The simplified formulation of this equation is reported here:

243
$$K = B * \Phi_{eff}^n \quad [2]$$

244 Where:

245 K = saturated hydraulic conductivity

246 B, n = fitting parameters

247 Φ_{eff} = effective soil porosity hydraulically active at saturation

248 Jarvis et al. (2002) extended the application of the equation [2] to the near-saturated hydraulic
249 conductivity. According to these applications, equation [2] has been applied here to the
250 different values of near-saturated hydraulic conductivity measured at different tensions
251 separately. The equation has been applied in the form:

252
$$K(h) = B_h * \Phi_{eff}^{n_h} \quad [3]$$

253 h = water tension at which K(h) has been referred (kPa)

254 K(h) = near-saturated hydraulic conductivity (cm s⁻¹) referred at h

255 B_h, n_h = fitting parameters

256 Φ_{eff} = effective soil porosity hydraulically active at saturation

257 Effective porosity is described using different limits of water tensions by different authors
258 (Ahuja et al., 1984; Messing, 1989; Rawls et al., 1998; Poulsen et al., 1999; Han et al., 2008)
259 as pore-size distributions and water retention curves vary across soils and over time. We
260 decided to fit the total porosity in equation [3] instead of effective porosity, assuming that the
261 reduction of porosity between total and effective will be expressed by an average proportion
262 that will be included in the B_h fitted parameter. This decision was justified by the fact that we
263 worked on only one type of soil and was also supported by the good curve fitting we obtained
264 that is presented later.

265
$$K(h) = B_h * \Phi^{n_h} \quad [4]$$

266 According to Aimrun et al. (2004), equation [4] also bears similarities to expressions relating
267 unsaturated hydraulic conductivity to the degree of saturation as presented by Averjanov

268 (1950), Wyllie and Spangler (1952), and Brooks and Corey (1964). Consequently, the four
269 regressions, each applied to a different water tension, could be combined into one as long as
270 the reduction of water-filled pore space at those different water tensions is taken into
271 account.

272 Differences in both parameters B_h and n_h at each water tension were tested at a 95%
273 confidence interval of probability; at significant differences, non-linear regression was applied
274 to express the variation as a function of the water tension.

275 The goodness of fit between estimated and measured values of near-saturated hydraulic
276 conductivity was checked through the coefficient of determination R^2 , the NRMSE (Loague
277 and Green, 1991), and by regression analysis between fitted and measured values. The null
278 hypothesis tested was that the linear regression did not significantly deviate from the 1:1 line.
279 These statistics were applied to log transformed near-saturated hydraulic conductivity data as
280 previously specified.

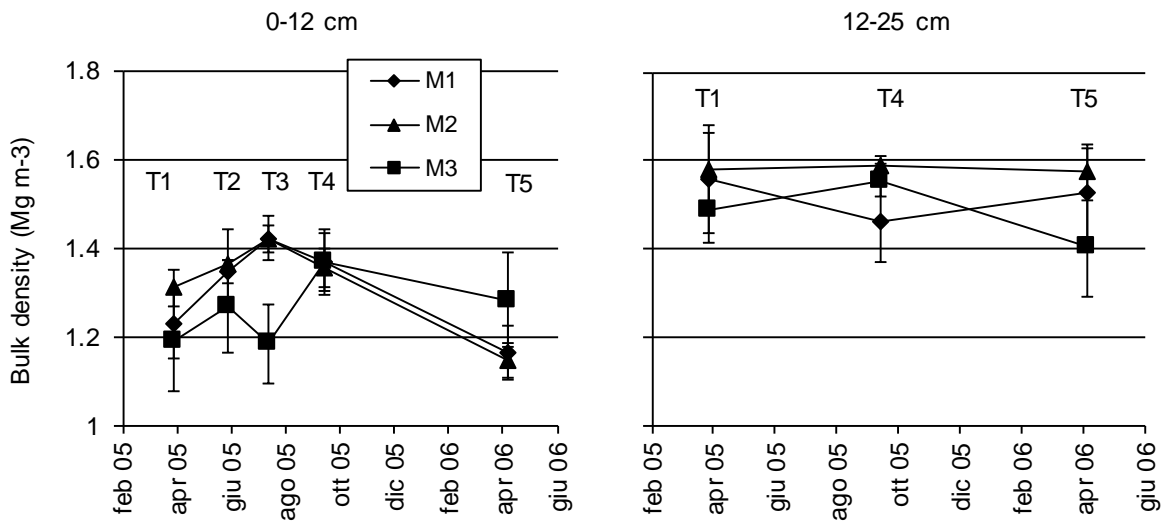
281 3 Results

282 3.1 Seasonal variations

283 3.1.1 Bulk density

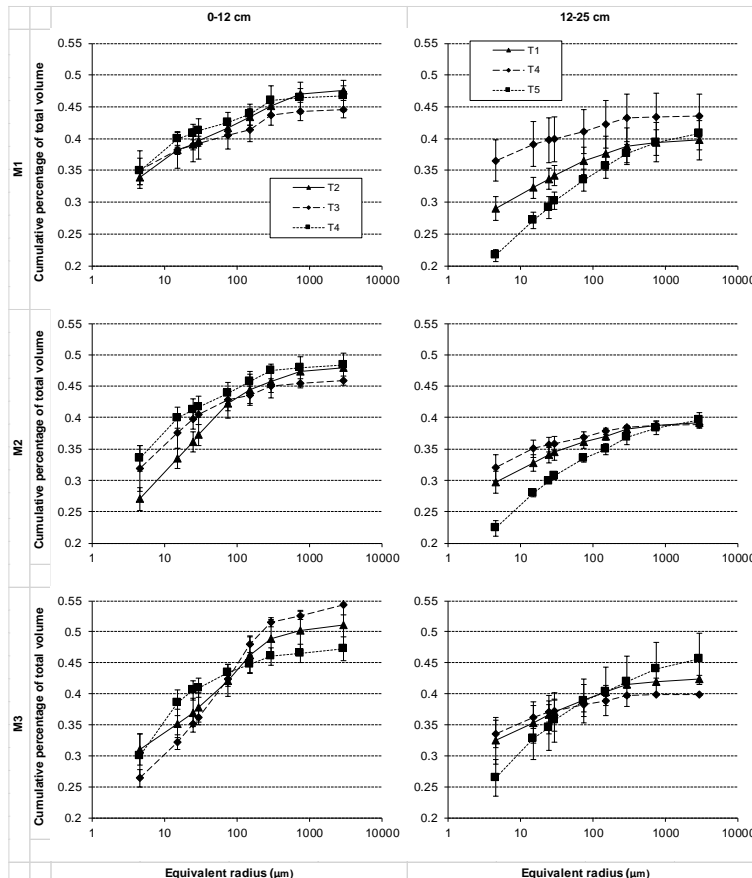
284 In the first layer, the general trend of the bulk density is to increase from T1 to T3 and then
285 decreases from T3 to T5 (Figure 2). In the interval between T1 and T2, the average bulk
286 density values increased in M1 to a greater extent than compared to the other two treatments;
287 they increased to the same extent. In the T2-T3 interval, bulk density increased in both of the
288 submerged treatments to the same extent while it decreased in M3 due to the weeding and
289 ridging performed. During the last part of the cropping season, bulk density decreased in M1
290 and in M2 due to submerging water removal while it increased in never-submerged M3. At
291 this point in the process, the three treatments showed the same value of bulk density. At T5
292 bulk density values were equal for M1 and M2 and greater for M3.

293 Fig. 2: Bulk density of the three managements measured at different times in the two layers.
 294 Error bars refer to 95% confidence interval.



295
 296 Second layer values showed greater pattern variability; however, the values at the beginning
 297 of the second year were close to those at the beginning of the first year, except for M3.

298
 299 Fig. 3: Cumulative pore size distribution curves of the three different managements measured
 300 at different times. Larger values are referred to an arbitrary pore radius as they represent the
 301 saturation. Error bars refer to 95% confidence interval.



303 3.1.2 Cumulative pore size distribution curve

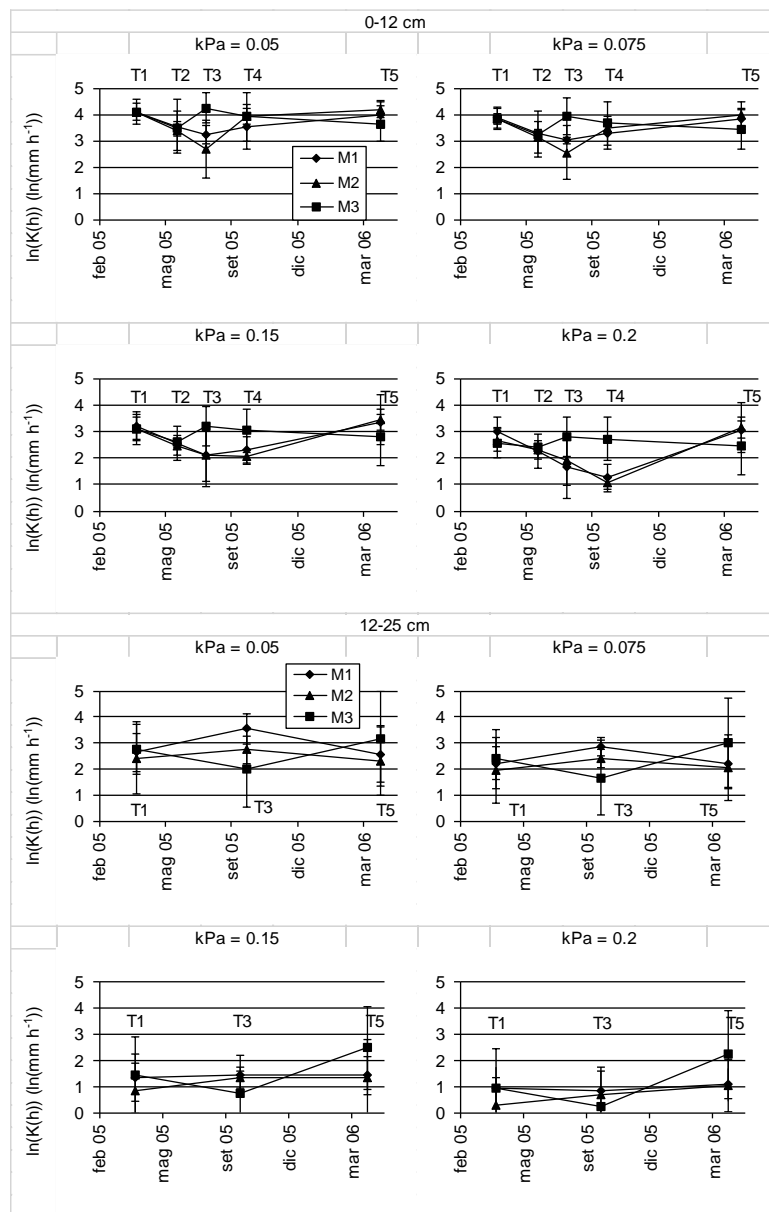
304 Figure 3 shows the cumulative pore size distribution curve of the three treatments at different
305 sampling times of the two layers. Larger values are referred to an arbitrary pore radius as they
306 represent the saturation. In the first layer of the submerged treatments (M1, M2) from T2 to
307 T3, the cumulative pore size distribution curve decreased in macro- and meso-porosity
308 volume and increased in micro-porosity volume. The increase is more evident in M2 than in
309 M1. During the T3 - T4 interval, the porosity increased in all the explored ranges. In the case
310 of M3, the behaviour of the ranges of porosity was different. Macro- and meso-porosity
311 increased from T2 to T3 due to the effect of ridging and weeding while micro-porosity
312 decreased. In the later interval, the opposite occurred.

313 In the second layer of the submerged treatments, the porosity increased from T1 to T4. Later,
314 during T5, it decreased. The same result occurred in M3 for micro-porosity, but the behaviour
315 was reversed for macro- and meso-porosity.

316

317

318 Fig. 4: Near-saturated hydraulic conductivity of the three different managements measured at
 319 different times. Error bars refer to 95% confidence interval.
 320



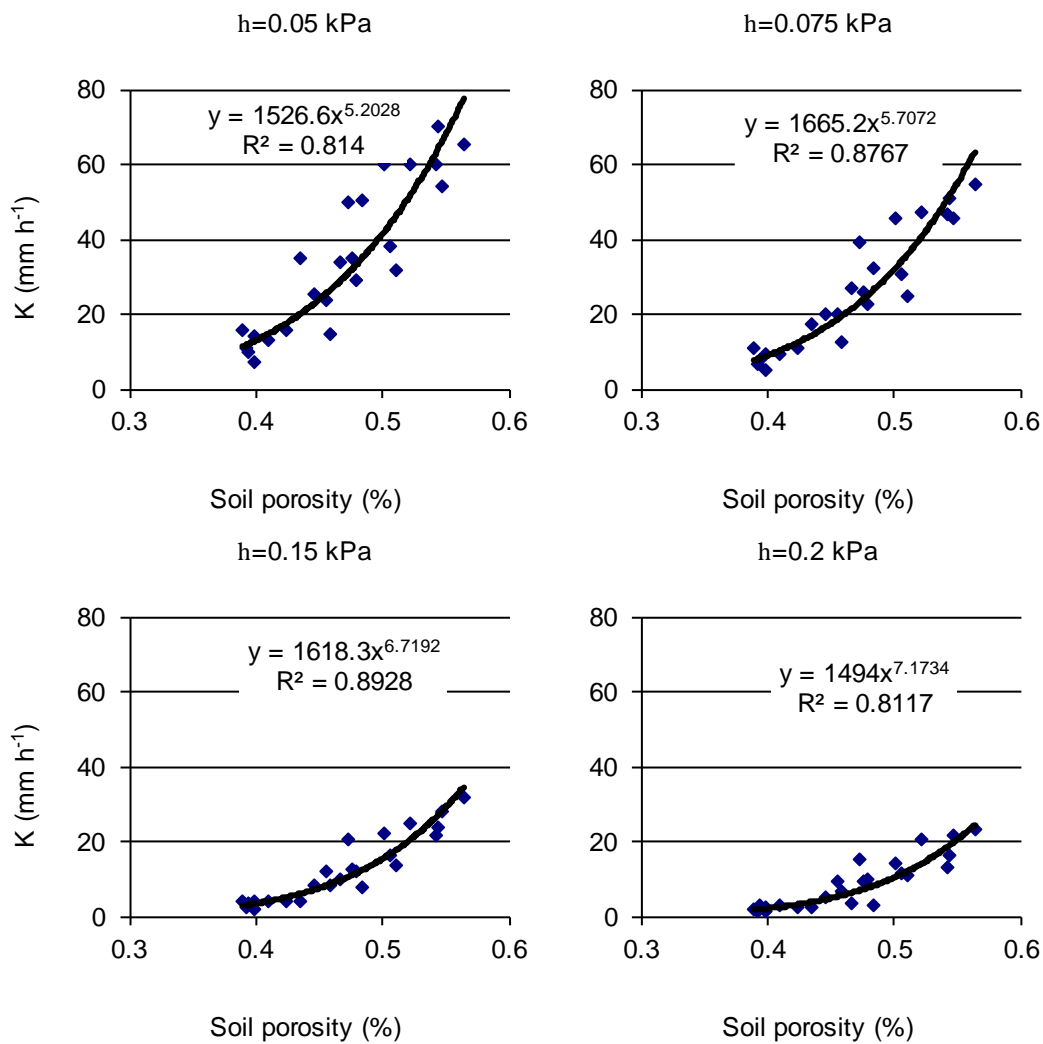
321
 322 3.1.3 Near-saturated hydraulic conductivity
 323 Figure 4 reports near-saturated hydraulic conductivity. The results partly confirmed the trend
 324 shown for bulk density; that is, all values in the first layer at T1 were similar for all treatments
 325 save for M2 that instead showed some bulk density differences. Between T3 and T4, as a
 326 consequence of drainage, the near-saturated hydraulic conductivity increased at the two
 327 greater tensions while it decreased at the lower tension. During this interval the increase in

328 soil porosity has increased the near-saturated hydraulic conductivity only at tensions closer to
329 saturation showing a different behaviour than at the other times of measurements. At T5,
330 values were equal to those at T1 for M1 and M2, and in agreement with bulk density
331 measurements. Among them, the value for M3 was the greatest.

332 In the second layer, trends in M1 and M2 were quite homogeneous as opposed to the increase
333 in near-saturated hydraulic conductivity at the greater tensions seen in M3 at T3.

334

335 Fig. 5: Relationship between near-saturated hydraulic conductivity measured at different
336 water tensions and total porosity (n = 24). All treatments x dates x depth are pooled together.
337



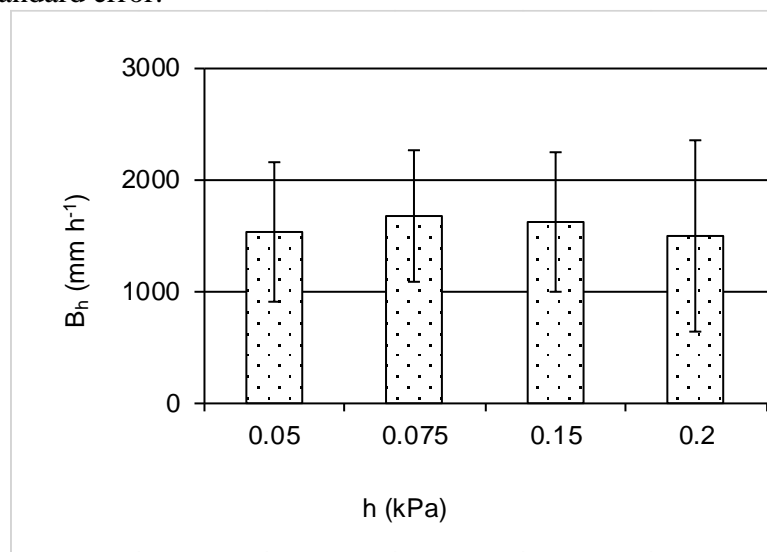
338

339 3.2 Porosity—near-saturated hydraulic conductivity relationship

340 Equation [4] has been applied to near-saturated hydraulic conductivity, measured at different
341 water potentials, and total porosity (Figure 5) using the dataset obtained by pooling together
342 times, managements, and depths. It shows good coefficients of determination ranging from
343 0.812 to 0.893.

344

345 Fig. 6: Values of the fitted parameter B_h of equation [4] at different water tensions (h). Error
346 bars represent standard error.



347

348

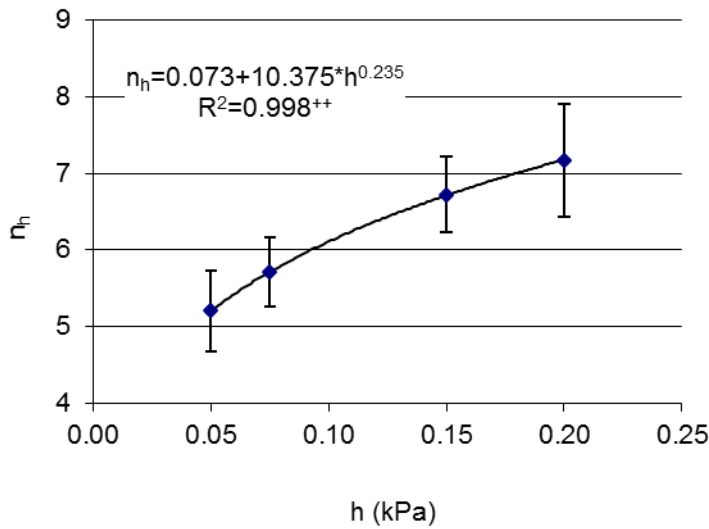
349 Figure 6 represents the B_h fit parameter of equation [4] reported in Figure 5 at water tensions
350 0.05, 0.075, 0.15, and 0.2 kPa. The B_h values showed little variability and no statistical
351 differences between different water tensions. This confirms what Ahuja (1984) reported—
352 that B is a specific parameter of the soil.

353 Figure 7 represents the n_h parameter of the equation. In contrast to B_h , n_h shows important
354 differences relative to the water tensions and an increasing trend as the soil gets drier. The
355 data represented on the graph correspond to the four values of water tension and were fitted
356 with an empirical function in the same mathematical form as that of the Kozeny Carman

357 equation, albeit with the addition of a constant to maintain proportionality between K and Φ
 358 even when h was equal to zero.

359

360 Fig. 7: Values of the fitted parameter n_h of equation [4] at different water tensions (h). Error
 361 bars represent standard error.
 362



363

364 The fitted equation for n is reported below:

$$365 \quad n_h = m + C \cdot h^d \quad [5]$$

366 The fitting of the power function equation [5] resulted in a highly significant non-linear
 367 regression and a coefficient of determination very close to 1 (Figure 7). We are aware that
 368 only four points (one for each tension) have been fitted, however the n_h parameter follows
 369 very well the equation that is expected to describe the progressive reduction of conductive
 370 porosity as water tension increases.

371 When equations [4] and [5] are joined, we obtain equation [6]:

$$372 \quad K(h) = B_h * \Phi^{m+C*h^d} \quad [6]$$

373 that can also be expressed in the more simple logarithmic form used for the fitting:

$$374 \quad \ln(K(h)) = \ln(B_h) + (m + C * h^d) * \ln(\Phi) \quad [7]$$

375 Where:

376 h = water tension at which $K(h)$ has been referred (kPa),
 377 $K(h)$ = near-saturated hydraulic conductivity referred at h (cm s^{-1}),
 378 B_h, C, m, d = fitting parameters, and
 379 Φ = total soil porosity.
 380 Equation [7] lets us summarize the four equations [4] into only one, and consequently reduce
 381 the total number of parameters from eight (two for each of the four tension-specific equations
 382 [4]) to four, and increase the number of cases to 96 (pooled dataset).
 383 Equation [6] is a new semi-empirical description of the relationship that relates near-saturated
 384 hydraulic conductivity to total porosity.
 385
 386 Fig. 8: Predicted values of the logarithm of the near-saturated hydraulic conductivity versus
 387 measured values with (a) or without (b) values measured in T4 as specified in the text.



389 Figure 8a shows the final results of the fitting. The relationship between measured and
390 predicted values of the logarithm of the near-saturated hydraulic conductivity is very good
391 with a coefficient of determination greater than 0.9 and a RMRSE equal to 11%, but with a
392 significant deviation with respect to a 1:1 line that led to a slight overestimation close to the
393 saturation.

394

395 4 Discussion

396 4.1 Seasonal variations

397 Most treatments, if submerged the year before the measurements, showed a value of bulk
398 density close to 1.18 Mg m^{-3} . Also the treatment cultivated with maize, but submerged during
399 the previous year, showed the same value in T1 as well as after weeding and ridging.
400 Consequently it can be assumed that this soil, if submerged during the previous year, tends to
401 reach a constant value of BD after secondary tilling. Moret and Arrùe (2007b) have also
402 described this very low variability in bulk density measured under the same conditions but in
403 different years or at different points in time, albeit for a different soil type.

404 After tilling, the physical properties of soil start their dynamics. The effect of the water on the
405 soil from irrigation or water submersion tends to decrease the porosity and the water
406 permeability (Kukal and Aggarwal, 2002; Cameira et al., 2003). The results of this
407 experiment allowed us to quantify the effect of the rainfall and the effect of the submerging
408 water.

409 During the interval T1-T3, M1 was constantly submerged and the bulk density increased for
410 97 days (not accounting for 5 days when the soil was drained). Assuming a constant rate, this
411 corresponds to approximately $2 \text{ kg m}^{-3} \text{ d}^{-1}$. Obviously, it is expected that the process reaches a
412 plateau, but the measured data do not permit us to define when this occurs. The M2 treatment

413 was submerged during the T2-T3 interval as well, and the measured rate of increase in bulk
414 density confirmed the rate calculated in M1.

415 The increase of bulk density in M2 and M3 during the T1-T2 interval and in M3 during the
416 T3-T4 interval was mainly driven by rainfall between other processes. During the second
417 interval, total rainfall was equal to 454.8 mm which led to a greater rate of compaction when
418 compared with those calculated in the first period for both treatments when only 135.4 mm of
419 rain fell. The effect of the almost-permanent submerging water on soil compaction was
420 greater than the effect exerted by 135.4 mm of rainfall and comparable to the effect of 454.8
421 mm.

422 After the removal of the submerging water in M1 and M2, the soil drainage and root turnover
423 (Cameira et al., 2003) created a new porosity and a decrease in bulk density.

424 The water retention curve allows us to better understand which pore dimensions contribute
425 most to total porosity at different times. The effect exerted by water trough submersion or
426 rainfall tends to disrupt macro- and meso-porosity and this is evident either in the treatment
427 submerged or not submerged during the first interval.

428 The second effect exerted by the water is the increase in micro-porosity that can be noted in
429 M2 during the T2-T3 interval (T2: beginning of submersion). In M1 it seems that the increase
430 happened before T2 as at this time, micro-porosity values were almost equal to those of T3.
431 As M2 was submerged only after T2, and M1 was already submerged before T2, the
432 comparison of these two different situations reveals that whereas the process of reduction in
433 macro- and meso-porosity due to water submersion continues for a long time, the process of
434 creation of micro-porosity after laser levelling is very fast and is shorter than the interval T1-
435 T2 or T2-T3.

436 In T4 water drainage and root turnover caused an increase in porosity in all explored ranges of
437 pores.

438 In M3, the effect of tillage between T2 and T3 increased the macro- and meso-porosity as
439 expected, but also reduced the micro-porosity. After T3 the soil was not disturbed other than
440 by rainfall that resulted in the same effect as that produced by irrigation of the submerged
441 treatment during the T2-T3 interval (macro- and meso-porosity decreased and micro-porosity
442 increased).

443 Hu et al. (2009) analysed the trend of the different pore classes over time in relation to
444 different rainfed crops, and expressed results in terms of contribution to water flow. They
445 described trends similar to those described in this work between T1 and T3, with a
446 progressive reduction of the role of the macro- and meso-porosity during the growing season
447 and an increase of the role of the micro-porosity. However, they failed to note any new
448 increase of macro- and meso-porosity at the end of the growing season, nor any reduction in
449 bulk density. In contrast, Cameira et al., (2003) reported an increase of macro- and meso-
450 porosity at the end of the growing season. Consequently, it is clear that different soils behave
451 differently in this respect.

452 The results seen in the near-saturated hydraulic conductivity of the first layer confirmed the
453 trend shown in bulk density. The three treatments at the onset of the experiment and M1 and
454 M2 at the beginning of the second year showed very similar values due to a common history.
455 M3 instead demonstrated different values due to a different history of submersion.

456 It is interesting to note that at T4, the near-saturated hydraulic conductivity at water tensions
457 greater than 0.15 kPa followed a different pattern when compared to the other tensions and to
458 the trend measured in bulk density. The interruption of the submersion, with a consequent
459 drying of the soil, changed the near-saturated hydraulic conductivity curve and its relationship
460 to bulk density.

461 The increase in macro- and meso-porosity measured in the T3-T4 interval led to a greater
462 near-saturated hydraulic conductivity only at water tensions greater than 0.15 kPa. In fact,

463 near-saturated hydraulic conductivity at 0.15 kPa remained almost constant while it decreased
464 at 0.20 kPa. This confirms that, as expected, the near-saturated hydraulic conductivity is
465 dominated by the larger pore classes.

466 In the second layer, the most interesting aspect is related to the effect of the laser levelling. It
467 was performed before T1 but not before T5. As shown by the water retention curves, macro-
468 and meso-porosity is similar in the two situations, which reveals the minor effect laser
469 levelling plays on this porosity range. Moreover, micro-porosity is greater at T1 than in T5,
470 showing that many other environmental effects can influence micro-porosity more than laser
471 levelling can.

472 The very similar pattern observed over time between macro- and meso-porosity and near-
473 saturated hydraulic conductivity measured at water tensions greater than 0.15 kPa also
474 confirmed the simple relationship that exists between these two soil physical characteristics.

475

476 4.2 Porosity —near-saturated hydraulic conductivity relationship

477 The relationship between the near-saturated hydraulic conductivity measured to 0.2 kPa of
478 water tension and total porosity explained most of the combined seasonal variation of the two
479 parameters. It showed that near-saturated hydraulic conductivity could be derived from total
480 porosity after the equation was parameterised. The unique equation showed that the relative
481 distribution of different pore classes is quite constant in the soil despite different depths,
482 treatments, and situations during the year.

483 The overestimation of the near-saturated hydraulic conductivity that we obtained close to
484 saturation from fitting equation [6] derived from the different behaviour of near saturated
485 hydraulic conductivity measured at water tensions greater than 0.15 kPa in T4 as previously
486 underlined. Removing the values measured in T4 from the regression, the new coefficients of
487 determination for the regressions (shown in figure 5) would increase to about 90%, which

488 would allow them to still be fitted by equation [4] with similar results. B_h values would still
489 not be statistically different between water tensions. A new fitting performed on equation [6]
490 would yield a final coefficient of determination increased to 95%, the NRMSE would
491 decrease to 7.6%, and the regression would become statistically not different from the 1:1 line
492 (Figure 8b) perfectly describing the relationship to all the other times of measurement.

493

494 5 Conclusions

495 The total amount and the relative distribution of the different pore classes in the ploughed
496 layer show an important dynamic over the cropping season that leads to quite different values
497 of bulk density, water retention curves, and near-saturated hydraulic conductivity.
498 Hydrological and biochemical processes that depend on these parameters require a
499 characterization over time of the soil physical properties that must take seasonal variation into
500 account. Submerging water and rainfall both destroy macro- and meso-porosity while on the
501 other hand, micro-pores are formed.

502 The strict relationship between near-saturated hydraulic conductivity and bulk density
503 described in this soil led to development of a semi-empirical model that could describe the
504 near-saturated hydraulic conductivity *versus* total porosity dynamic at any time interval. This
505 let measure the latter soil physical property with a lower intensity of bulk density.

506 Coupled measurements of near-saturated hydraulic conductivity and bulk density performed
507 after the final soil drainage showed a behaviour different from the rest of the dataset and
508 should be further investigated. Also the equation relating porosity to near-saturated hydraulic
509 conductivity should be tested and validated over a wider range of soils.

510

511 Acknowledgments

512 The Authors thank Simone Pelissetti, Monica Bassanino, and Delia De Stefano for helping in
513 the fieldwork and Joan Leonard for the English revision of the manuscript. The project has
514 been partially financed by Regione Piemonte, Assessorato all'Agricoltura e foreste e alla
515 Caccia e pesca and by the European project UNISEB: Improvement of skills for managing
516 high quality sustainable agro food production 2003-2007.

517

518 **References**

519 Ahuja, L.R., Naney, J.W., Green, P.E., Nielsen, D.R., 1984. Macroporosity to characterise
520 spatial variability of hydraulic conductivity and effects of land management. *Soil Sci. Soc.*
521 *Am. J.*, 48, 699-702.

522 Aimrun, W., Amin, M.S.M., Eltaib, S.M., 2004. Effective porosity of paddy soils as an
523 estimation of its saturated hydraulic conductivity. *Geoderma*, 121, 197-203.

524 Ankeny, M.D., M. Ahmed, T.C. Kaspar, and R. Horton. 1991. Simple field method for
525 determining unsaturated hydraulic conductivity. *Soil Sci. Soc. Am. J.*, 55: 467-470.

526 Averjanov, S.F., 1950. About Permeability of Subsurface Soils in Case of Incomplete
527 Saturation. *Eng. Collect.* 7, as quoted by P. Ya. Polubarinova Kochina, *The Theory of Ground*
528 *Water Movement*, English Translation by J.M. Roger De Wiest, 1962. Princeton Univ. Press,
529 Princeton, NJ.

530 Blake, G.R., and K.H. Hartge. 1986a. Particle density. p. 377–382. In A. Klute (ed.) *Methods*
531 *of soil analysis. Part 1.* 2nd ed. ASA and SSSA, Madison, WI.

532 Blake, G.R., and K.H. Hartge. 1986b. Bulk density. p. 363-375. In: *Methods of soil analysis -*
533 *Part 1: Physical and mineralogical methods (2nd edition)*, Am. Soc. of Agronomy and Soil Sci.
534 *Soc. Am. Publ.*, Madison, Wisconsin.

535 Bormann, H., Klaassen, K., 2008. Seasonal and land use dependent variability of soil
536 hydraulic and soil hydrological properties of two Northern German soils. *Geoderma*, 145,
537 295-302.

538 Brooks, R.H., Corey, A.T., 1964. Hydraulic properties of porous media. Hydrology Paper no.
539 3, Colorado State University, Fort Collins, CO.

540 Cameira, M.R., Fernando, R.M., Pereira, L.S., 2003. Soil macropore dynamics affected by
541 tillage and irrigation for a silty loam alluvial soil in southern Portugal. *Soil Till. Res.*, 70,
542 131–140.

543 Carman, P.C., 1937. Fluid flow through granular beds. *Trans. Inst. Chem. Eng. Lond.* 15,
544 150-166.

545 Carman, P.C., 1956. *Flow of Gases Through Porous Media*. Academic Press, New York.

546 Daraghmeh, O. A., Jensen, J. R., Petersen, C. T., 2008. Near-Saturated Hydraulic Properties
547 in the Surface Layer of a Sandy Loam Soil under Conventional and Reduced Tillage. *Soil Sci.*
548 *Soc. Am. J.*, 72, 6, 1728-1737.

549 EMBRAPA, 1997. *Manual de métodos de análise de solo*. Centro Nacional de Pesquisa de
550 Solo. 2.ed. Rio de Janeiro: EMBRAPACNPS, 212p.

551 Gardner, W., Jury, W.A., Gardner, W.H., 1991. *Soil Physics*, 5th Edition. John Wiley &
552 Sons, Inc., pages 328.

553 Han, H., Giménez, D., Lilly, A., 2008. Textural averages of saturated soil hydraulic
554 conductivity predicted from water retention data. *Geoderma*, 146, 121–128.

555 Hu, W., Shao, M., Wang, Q., Fan, J., Horton, R., 2009. Temporal changes of soil hydraulic
556 properties under different land uses. *Geoderma* 149, 355-366.

557 Jarvis, N.J., Zavattaro, L., Rajkai, K., Reynolds, W. D., Olsen, P. A., McGechan, M., Mecke,
558 M., Mohanty, B., Leeds-Harrison, P. B., Jacques. D., 2002. Indirect estimation of near-

559 saturated hydraulic conductivity from readily available soil information. *Geoderma*, 108(1-2),
560 1-17.

561 Juma, N. G. 1993. Interrelationships between soil structure/texture, soil biota/soil organic
562 matter and crop production. *Geoderma* 57, 3-30

563 Klute, A. 1986. Water retention: laboratory methods. p. 635-662. In: *Methods of soil analysis*
564 - Part 1: Physical and mineralogical methods (2nd edition), Am. Soc. of Agronomy and Soil
565 Sci. Soc. Am. Publ., Madison, Wisconsin.

566 Kozeny, J., 1927. Ueber Kapillare Leitung des Wassers in Boden. *Sitzungsber., Akad, Der*
567 *Wissensch, Wien, Math.-naturw. Klass. Abt. Ila* 136, 271-306.

568 Kukal, S.S., Aggarwal, G.C., 2002. Percolation losses of water in relationshipship to
569 puddling intensity and depth in a sandy loam rice (*Oryza sativa*) field. *Agricultural Water*
570 *Management*, 57, 49–59.

571 Kutilek, M., 2004. Soil hydraulic properties as related to soil structure. *Soil Till. Res.*, 79,
572 175–184.

573 Kutilek, M., Jendele, L., Panayiotopoulos, K.P., 2006. The influence of uniaxial compression
574 upon pore size distribution in bi-modal soils. *Soil Till. Res.*, 86, 27–37.

575 Loague, K.M., Green, R.E., 1991. Statistical and graphical methods for evaluating solute
576 transport models: overview and application. *Journal of Contaminant Hydrology*, 7, 51-53.

577 Luxmoore, R.J., 1981. Micro-, meso- and macro-porosity of soil. *Soil Sci. Soc. Am. J.*, 45,
578 241–285.

579 Messing, I., 1989. Estimation of saturated hydraulic conductivity in clay soils from moisture
580 retention data. *Soil Sci. Soc. Am. J.*, 53, 665–668.

581 Messing, I., Jarvis, N.J., 1993. Temporal variation in the hydraulic conductivity of a tilled
582 clay soil as measured by tension infiltrometers. *J. Soil Sci.* 44, 11 –24.

583 Mohanty, M., Painuli, D., Mandal, K., 2004. Effect of puddling intensity on temporal
584 variation in soil physical conditions and yield of rice (*Oryza sativa* L.) in a Vertisol of central
585 India. *Soil Till. Res.* 76, 83-94.

586 Moret, D., Arrùe, J.L., 2007a. Characterizing soil water-conducting macro- and mesoporosity
587 as influenced by tillage using tension infiltrometry. *Soil Sci. Soc. Am. J.*, 71, 2, 500–506.

588 Moret, D., Arrùe, J.L., 2007b. Dynamics of soil hydraulic properties during fallow as affected
589 by tillage. *Soil and Tillage Research* 96, 103-113.

590 Pagliai, M., De Nobile, M., 1993. Relationships between soil porosity, root development
591 and soil enzyme activity in cultivated soils. *Geoderma*, 56, 243-256

592 Pagliai, M., Vignozzi, N., 2002. Image analysis and microscopic techniques to characterize
593 soil pore system. In: Blahovec, J., Kutilek, M., (Eds.), *Physical Methods in Agriculture*.
594 Kluwer Academic Publishers, London, 13–38.

595 Petersen, C.T., Trautner, A., Hansen, S., 2004. Spatio-temporal variation of anisotropy of
596 saturated hydraulic conductivity in a tilled sandy loam soil. *Soil and Tillage Research* 100,
597 108-113.

598 Poulsen, T.G., Moldrup, P., Yamaguchi, T., Jacobsen, O.H., 1999. Predicting saturated and
599 unsaturated hydraulic conductivity in undisturbed soils from soil water characteristics. *Soil*
600 *Sci.* 164, 877–887.

601 Rawls, W.J., Gimenez, D., Grossman, R., 1998. Use of soil texture, bulk density, and slope of
602 the water retention curve to predict saturated hydraulic conductivity. *Trans. ASAE* 41, 983–
603 988.

604 Schwartz, R.C., Evett, S.R., Unger, P.W., 2003. Soil hydraulic properties of cropland
605 compared with reestablished and native grassland. *Geoderma* 116, 47-60.

606 SIA, 2000. *Analisi chimiche e fisiche del suolo*. Milano, Società Italiana di Agronomia, v.2.
607 2013 p.

608 USDA, 1977. Keys to Soil Taxonomy. Soil Survey Staff, Soil Conservation Service U.S.
609 Dept. Of Agriculture, 7th edition, Pocahontas Press, Inc., Virginia, Usa, pp. 545.

610 White, I., M.J. Sully, and K.M. Perroux. 1992. Measurement of surface-soil hydraulic
611 properties: disk permeameters, tension infiltrometers, and other techniques. p. 69–103. In
612 G.C. Topp et al. (ed.) Advances in measurement of soil physical properties: Bringing theory
613 into practice. SSSA Spec. Publ. 30, SSSA, Madison, WI.

614 Wyllie, M.R.J., Spangler, M.B., 1952. Application of electrical resistivity measurements to
615 problem of fluid flow in porous media. Bull. Am. Assoc. Pet. Geol. 36, 359– 403.

616 Zavattaro, L., Grignani, C., 2001. Deriving Hydrological Parameters for Modeling Water
617 Flow under Field Conditions. Soil Sci. Soc. Am. J., 65, 655–667.

618 Zavattaro, L., Jarvis, N, Persson, L., 1999. Use of Similar Media Scaling to Characterize
619 Spatial Dependence of Near-Saturated Hydraulic Conductivity. Soil Sci. Soc. Am. J., 63, 486-
620 492.